IEEE Access
Multidisciplinary | Rapid Review | Open Access Journal

Received October 22, 2018, accepted November 11, 2018, date of publication November 26, 2018,
date of current version January 7, 2019.

Digital Object Identifier 10.1109/ACCESS.2018.2883405

Terminal Guidance Based on Bézier Curve for Climb-and-Dive Maneuvering Trajectory With Impact Angle Constraint

ZHEN QIN, XIAOYE QI, AND YONGLING FU
School of Mechanical Engineering and Automation, Beihang University, Beijing 10083, China
Corresponding author: Yongling Fu (fuyongling@buaa.edu.cn)

This work was supported by the National Natural Science Foundation of China under Grant 61327807.

ABSTRACT To improve the penetration capability and the damage effectiveness of cruise missiles, maneuvering trajectory with specific impact angle is applied in terminal guidance. In this paper, an innovative online method for terminal guidance is presented, which can guide the cruise missile to a stationary target along a climb-and-dive maneuvering trajectory while meeting the expected impact angle. The basic principles of the proposed guidance method are the Bézier curve theory and the missile inverse dynamics. The maneuvering trajectory is shaped by a third-order Bézier curve based on the missile current state, the target position, and the impact angle constraint. The real-time guidance command represented by attack angle α is obtained based on the missile inverse dynamics. The shape of flight trajectory can be modified by regulating the Bézier parameters b_1 and b_2 to satisfy different tactical requirements without changing the boundary conditions. Simulation results demonstrate the effectiveness of the proposed method applied in cruise missile terminal guidance.

INDEX TERMS Cruise missile, terminal guidance, maneuvering trajectory, impact angle, Bézier curve.

I. INTRODUCTION

Cruise missiles play an important role in modern warfare due to their advantages of small size, low cost, high precision, and high maneuverability. However, the survival of cruise missiles has become increasingly severe with the developments of anti-missile systems [1]. Planning climb-and-dive maneuvering trajectory, especially at the terminal guidance phase, can improve the penetration capability of the missile and reduce the interception probability. In addition, some tactical tasks require the missile to attack the target with a specific impact angle to improve the damage effectiveness [2], [3].

Previous researchers conducted a series of work on missile terminal guidance. To achieve the climb-and-dive maneuvering trajectory, methods such as two-phase proportional navigation guidance law [4]–[6] and optimal guidance law [7]–[10] are applied before. The two-phase proportional navigation guidance assumes a transition point within the flight trajectory which divides the entire trajectory into two phases. At the first phase, the missile climbs from the start point until it reaches the transition point. Then at the second phase, the missile turns down and dives until it hits the target. To meet the expected impact angle, methods such as biased proportional navigation guidance law [11]–[14], optimal guidance law [15]–[17], model predictive static programming technique [18], [19], and sliding mode control theory [20]–[22] are applied before. But most of these methods only focus on solving one of the maneuvering trajectory or impact angle problems.

Thus, an innovative online method for terminal guidance is proposed here, which can guide the cruise missile to a stationary target along a climb-and-dive maneuvering trajectory while meeting the expected impact angle. The maneuvering trajectory is shaped by a third-order Bézier curve according to the missile current state, the target position, and the impact angle constraint. The real-time guidance command represented by attack angle α is obtained based on the missile inverse dynamics.

The rest of this paper is organized as follows: section II describes the guidance problem, section III introduces the guidance method, section IV shows the simulation results, and section V demonstrates the conclusions.

II. PROBLEM STATEMENT

A. GUIDANCE PROBLEM

The purpose of this paper is to present a terminal guidance method for cruise missile attacking a stationary target.

When the missile enters terminal guidance phase, it tracks along a climb-and-dive maneuvering trajectory and hits the target with the expected impact angle. The missile trajectory of terminal guidance is shown in Fig. 1.

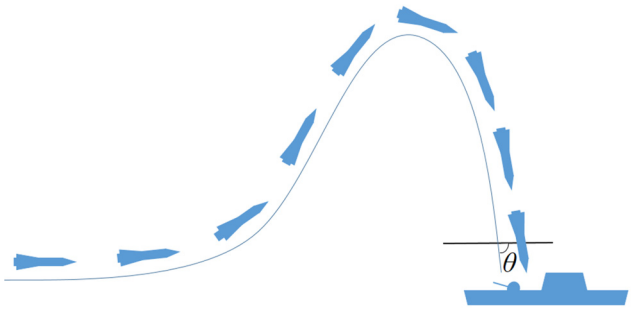

FIGURE 1. Climb-and-dive maneuvering trajectory with impact angle constraint.

B. MISSILE MOTION MODEL

The research object is a cruise missile moving in the vertical plane. A point mass missile and a flat non-rotating earth are assumed in this model. The forces, angles, and axes of the missile are defined in Fig. 2. The motion equations of the missile are shown in (1), where t (s) represents the flight time, x (m) represents the horizontal displacement, y (m) represents the vertical displacement, v (m/s) represents the velocity, θ (°) represents the flight path angle, α (°) represents the attack angle, n_y represents the normal overload, D (N) represents the drag, L (N) represents the lift, T (N) represents the engine thrust, g (m/s^2) represents the acceleration of gravity, m (kg) represents the mass, and m_c (kg/s) represents the rate of mass reduction.

$$\begin{aligned}\frac{dv}{dt} &= \frac{T\cos\alpha - D - mg\sin\theta}{m}\\ \frac{d\theta}{dt} &= \frac{T\sin\alpha + L - mg\cos\theta}{mv}\end{aligned}$$

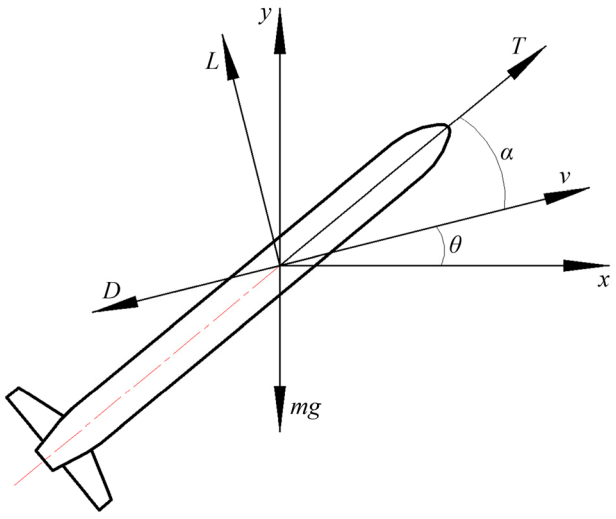

FIGURE 2. Definition of the missile motion variables.

$$\begin{aligned}\frac{dx}{dt} &= v\cos\theta\\ \frac{dy}{dt} &= v\sin\theta\\ \frac{dm}{dt} &= -m_c\\ n_y &= \frac{T\sin\alpha + L}{mg}.\end{aligned} \tag{1}$$

The constraints imposed on the attack angle and its derivative are shown in (2).

$$\begin{aligned}\alpha_{\min} \le \alpha \le \alpha_{\max}\\ |\dot{\alpha}| \le \dot{\alpha}_{\max}.\end{aligned} \tag{2}$$

The constraint imposed on the normal overload is shown in (3).

$$|n_y| \le n_{y\max}. \tag{3}$$

The drag D is expressed as (4), and the drag coefficient C_D is written as (5).

$$D = \frac{1}{2}SC_D\rho v^2, \tag{4}$$

$$C_D = A_1\alpha^2 + A_2\alpha + A_3. \tag{5}$$

The lift L is expressed as (6), and the lift coefficient C_L is written as (7).

$$L = \frac{1}{2}SC_L\rho v^2, \tag{6}$$

$$C_L = B_1\alpha + B_2. \tag{7}$$

S (m^2) represents the reference aerodynamic area of the missile. A_1, A_2, A_3, B_1, and B_2 are constants of drag and lift coefficients. Air density ρ (kg/m^3) is obtained from the standard atmospheric model (USA, 1976).

Table 1 shows the physical parameters of the missile [8], where m_0 (kg) represents the initial mass of the missile.

TABLE 1. Missile physical parameters.

Symbol	Value	Unit
S	0.3376	m^2
A_1	−1.9431	-
A_2	−0.1499	-
A_3	0.2359	-
B_1	21.9	-
B_2	0	-
T	5000	N
m_0	1005	kg
m_c	8	kg/s

III. GUIDANCE METHOD

Firstly, we shape the climb-and-dive maneuvering trajectory based on the Bézier curve theory, according to the missile current state, the target position, and the impact angle constraint. Secondly, we calculate the online guidance command based on the missile inverse dynamics.

A. TRAJECTORY SHAPED BY BÉZIER CURVE

Bézier curve was proposed by French engineer Pierre Bézier in 1962, who applied this kind of curve to automobile design. Since then, Bézier curve had been used in many fields, especially in computer graphic design and robot movement trajectory plan [23].

Bézier curve is ascertained by several control points. The control points include start point, terminal point, and a number of shape-define points. The order of Bézier curve depends on the number of control points. If the number of control points is n, the order is n−1. The curve passes through the start and terminal points, but does not necessarily pass through the shape-define points. That means the shape-define points can be moved to reshape and modify the curve without changing the initial and terminal boundary conditions. Each shape-define point can bend the curve once. More shape-define points can define a complex curve. For the given control points $P_0, P_1, P_2 ... P_n$, the Bézier curve can be written as a polynomial function of the parameter $\varepsilon \in [0,1]$, as shown in (8).

$$B(\varepsilon) = \sum_{i=0}^{n} \frac{n!}{i!(n-i)!} \varepsilon^i (1-\varepsilon)^{n-i} P_i. \tag{8}$$

For instance, third-order Bézier curve has four control points, as shown in Fig. 3. P_0 is the start point, P_1 and P_2 are the shape-define points, and P_3 is the terminal point. Once the positions of these control points are ascertained, the third-order Bézier curve is ascertained. Connect P_0, P_1, P_2, and P_3 with straight lines in turn. Q_0 moves on the line segment P_0P_1 from P_0 to P_1. Q_1 moves on the line segment P_1P_2 from P_1 to P_2. Q_2 moves on the line segment P_2P_3 from P_2 to P_3. Then connect Q_0, Q_1, and Q_2 with straight lines in turn. R_0 moves on the line segment Q_0Q_1 from Q_0 to Q_1. R_1 moves on the line segment Q_1Q_2 from Q_1 to Q_2. Then connect R_0 and R_1 with straight line. B moves on the line segment R_0R_1 from R_0 to R_1. The points Q_0, Q_1, Q_2, R_0, R_1, and B move on their own line segment respectively from the start point to the terminal point in pace with the parameter ε varies from 0 to 1, constrained by the ratio (9). The track of B generates the third-order Bézier curve. For example, when $\varepsilon = 0.25$, the position of B is shown in Fig. 3. The third-order Bézier curve polynomial function of ε is written as (10).

$$\frac{R_0B}{BR_1} = \frac{Q_0R_0}{R_0Q_1} = \frac{Q_1R_1}{R_1Q_2} = \frac{P_0Q_0}{Q_0P_1} = \frac{P_1Q_1}{Q_1P_2} = \frac{P_2Q_2}{Q_2P_3}. \tag{9}$$

$$B(\varepsilon) = (1-\varepsilon)^3 P_0 + 3\varepsilon(1-\varepsilon)^2 P_1 + 3\varepsilon^2(1-\varepsilon)P_2 + \varepsilon^3 P_3. \tag{10}$$

We select Bézier curve because it can completely define the missile trajectory by its start point, terminal point, and a finite number of shape-define points. The properties of Bézier curve are employed to enforce the initial, terminal, and path constraints of the trajectory. The curve passes through the start and terminal points, and shaped by the shape-define points. Therefore, reshaping the trajectory without changing the boundary conditions is convenient. This kind of curve helps to maintain the number of unknown parameters to a minimum compared with other methods [24].

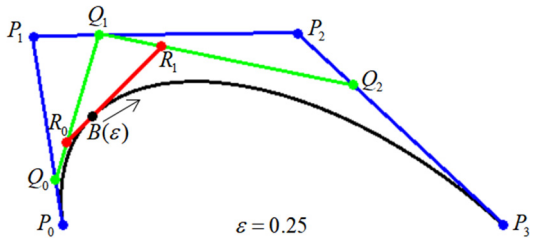

FIGURE 3. The third-order Bézier curve.

The climb-and-dive maneuvering trajectory has two turns: the first turn is between the horizontal cruising phase and the climbing phase, and the second turn is between the climbing phase and the diving phase. Therefore, at least a third-order Bézier curve with two shape-define points is applied in this situation to implement the two turns. The third-order Bézier trajectory with its four control points is shown in Fig. 4.

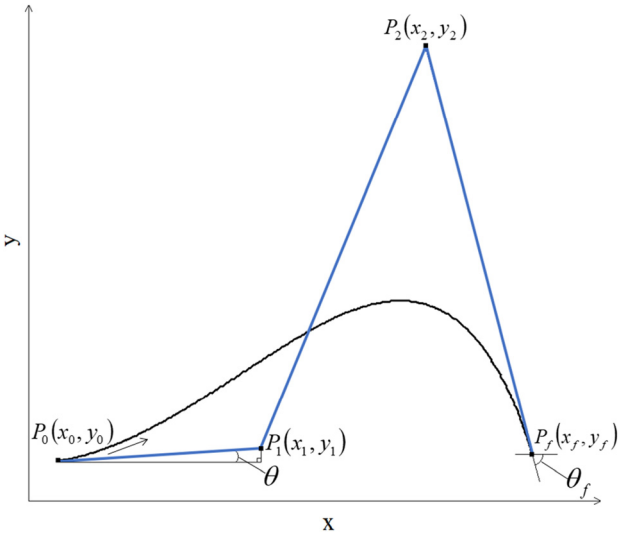

FIGURE 4. The third-order Bézier trajectory with its control points.

P_0 is the start point. P_f is the terminal point. P_1 and P_2 are the shape-define points which do not lay on the trajectory. If the positions of the two shape-define points are changed, the trajectory shape will be changed, while maintaining the same boundary conditions. P_1 lays on the tangent line of the trajectory at P_0, and P_2 lays on the tangent line of the trajectory at P_f. This geometry relationship ensures the initial and terminal conditions: $\tan\theta$ and $\tan\theta_f$. θ is the initial (current) flight path angle, and θ_f is the terminal flight path angle, as well as the impact angle.

According to (10), the coordinate of third-order Bézier curve can be written as a polynomial function of $\varepsilon \in [0,1]$, as shown in (11).

$$\begin{aligned} x &= (1-\varepsilon)^3 x_0 + 3\varepsilon(1-\varepsilon)^2 x_1 + 3\varepsilon^2(1-\varepsilon)x_2 + \varepsilon^3 x_f \\ y &= (1-\varepsilon)^3 y_0 + 3\varepsilon(1-\varepsilon)^2 y_1 + 3\varepsilon^2(1-\varepsilon)y_2 + \varepsilon^3 y_f. \end{aligned} \tag{11}$$

To obtain the positions of shape-define points P_1 and P_2, the Bézier parameters b_1 and b_2 are introduced here. The definition of b_1 and b_2 is shown in (12). Boundary constraints $\tan\theta$ and $\tan\theta_f$ can be expressed by the coordinate of control points, according to the geometric relationship, as shown in (13). Then the coordinate of shape-define points P_1 (x_1, y_1) and P_2 (x_2, y_2) can be expressed by the known parameters b_1, b_2, P_0 (x_0, y_0), P_f (x_f, y_f), θ, and θ_f, as shown in (14). The Bézier parameters b_1 and b_2 which set before the flight can define the shape of the climb-and-dive maneuvering trajectory. The values of b_1 and b_2 are obtained from a SQP (Sequential Quadratic Programming) method, which considers the constraints of attack angle and normal overload. Based on the missile current position P_0, the flight path angle θ, the target position P_f, and the expected impact angle θ_f, the reference Bézier trajectory can be updated and reshaped in real time in pace with the guidance cycle.

$$\begin{aligned} b_1 &= \frac{x_1 - x_0}{x_f - x_0} \\ b_2 &= \frac{x_2 - x_0}{x_f - x_0}. \end{aligned} \tag{12}$$

$$\begin{aligned} \tan\theta &= \frac{y_1 - y_0}{x_1 - x_0} \\ \tan\theta_f &= \frac{y_f - y_2}{x_f - x_2}. \end{aligned} \tag{13}$$

$$\left.\begin{aligned} x_1 &= b_1(x_f - x_0) + x_0 \\ y_1 &= \tan\theta(x_1 - x_0) + y_0 \end{aligned}\right\} \Rightarrow P_1(x_1, y_1)$$
$$\left.\begin{aligned} x_2 &= b_2(x_f - x_0) + x_0 \\ y_2 &= -\tan\theta_f(x_f - x_2) + y_f \end{aligned}\right\} \Rightarrow P_2(x_2, y_2). \tag{14}$$

B. GUIDANCE COMMAND OBTAINED BY MISSILE INVERSE DYNAMICS

The guidance command represented by attack angle α is obtained based on the missile inverse dynamics, which can calculate α from the reference trajectory [1]. The Bézier curve provides a shape-dependent trajectory. Thus, it is necessary to reduce the missile time-dependent motion equations (1) to the shape-dependent (x) motion equations, as shown in (15).

$$\begin{aligned} \frac{dv}{dx} &= \frac{T\cos\alpha - D - mg\sin\theta}{mv\cos\theta} \\ \frac{d\theta}{dx} &= \frac{T\sin\alpha + L - mg\cos\alpha}{mv^2\cos\theta} \\ \frac{dy}{dx} &= \tan\theta. \end{aligned} \tag{15}$$

According to Fig. 2, the normal acceleration a_y (m/s^2) can be derived based on the forces exerted on the missile, as shown in (16).

$$a_y = \frac{T\sin\alpha + L}{m}. \tag{16}$$

According to the second formula of (15), the normal acceleration a_{yB} (m/s^2) can be derived based on the trajectory shape, as shown in (17).

$$a_{yB} = \left(\frac{d\theta}{dx}\right) v^2\cos\theta + g\cos\theta. \tag{17}$$

According to the third formula of (15), the current flight path angle θ can be obtained, as shown in (18).

$$\theta = \arctan\left(\frac{dy}{dx}\right). \tag{18}$$

The derivative of θ which used for calculating a_{yB} is derived, as shown in (19).

$$\frac{d\theta}{dx} = \left(\frac{d^2y}{dx^2}\right)\cos^2\theta. \tag{19}$$

Thus, the normal acceleration a_{yB} can be obtained, as shown in (20).

$$a_{yB} = \left(\frac{d^2y}{dx^2}\right) v^2\cos^3\theta + g\cos\theta. \tag{20}$$

To obtain (d^2y/dx^2), the first and second derivatives of x and y versus ε should be derived at first based on (11), as shown in (21) and (22).

$$\begin{aligned} \frac{dx}{d\varepsilon} &= -3(1-\varepsilon)^2x_0 + 3x_1(3\varepsilon^2 - 4\varepsilon + 1) \\ &\quad + 3x_2(-3\varepsilon^2 + 2\varepsilon) + 3\varepsilon^2x_f \\ \frac{dy}{d\varepsilon} &= -3(1-\varepsilon)^2y_0 + 3y_1(3\varepsilon^2 - 4\varepsilon + 1) \\ &\quad + 3y_2(-3\varepsilon^2 + 2\varepsilon) + 3\varepsilon^2y_f. \end{aligned} \tag{21}$$

$$\begin{aligned} \frac{d^2x}{d\varepsilon^2} &= 6(1-\varepsilon)x_0 + 6x_1(3\varepsilon - 2) + 6x_2(-3\varepsilon + 1) + 6\varepsilon x_f \\ \frac{d^2y}{d\varepsilon^2} &= 6(1-\varepsilon)y_0 + 6y_1(3\varepsilon - 2) + 6y_2(-3\varepsilon + 1) + 6\varepsilon y_f. \end{aligned} \tag{22}$$

Based on (21) and (22), the required first and second derivatives of y versus x can be obtained, as shown in (23) and (24).

$$\frac{dy}{dx} = \frac{dy/d\varepsilon}{dx/d\varepsilon}. \tag{23}$$

$$\frac{d^2y}{dx^2} = \frac{\dfrac{d^2y}{d\varepsilon^2} - \dfrac{d^2x}{d\varepsilon^2}\dfrac{dy/d\varepsilon}{dx/d\varepsilon}}{\left(\dfrac{dx}{d\varepsilon}\right)^2}. \tag{24}$$

Substituting the coordinate of P_0 (x_0, y_0), P_1 (x_1, y_1), P_2 (x_2, y_2), and P_f (x_f, y_f) into (24), (d^2y/dx^2) can be derived as a function of b_1, b_2, x_0, y_0, x_f, y_f, θ, θ_f, and ε, as shown in (25).

$$\frac{d^2y}{dx^2} = f(b_1, b_2, x_0, y_0, x_f, y_f, \theta, \theta_f, \varepsilon). \tag{25}$$

Assuming the normal acceleration a_y (16) and a_{yB} (20) be equal, the guidance command represented by attack angle α can be calculated from (26). Each moment during the flight, the reference Bézier trajectory is updated and reshaped based on the missile current state, the target position and the impact angle constraint. The guidance command applied to control the flight is the value of α at P_0, where $\varepsilon = 0$. The guidance command is updated in real time with each guidance cycle.

$$a_y = a_{yB} \Rightarrow \frac{T\sin\alpha + L}{m} = \left(\frac{d^2y}{dx^2}\right) v^2\cos^3\theta + g\cos\theta. \tag{26}$$

According to the derivation above, the terminal guidance procedure for climb-and-dive maneuvering trajectory with expected impact angle constraint is accomplished.

IV. NUMERICAL SIMULATION RESULTS

A. NUMERICAL SIMULATION OF THE PROPOSED METHOD

The proposed method is applied in cruise missile terminal guidance. The purpose is to guide the missile to a stationary target along a climb-and-dive maneuvering trajectory with a certain impact angle. MATLAB is used for the numerical simulation. Fig. 5 shows the simulation procedure. Table 2 shows the initial and terminal conditions. Table 3 shows the Bézier parameters b_1 and b_2 for different impact angles.

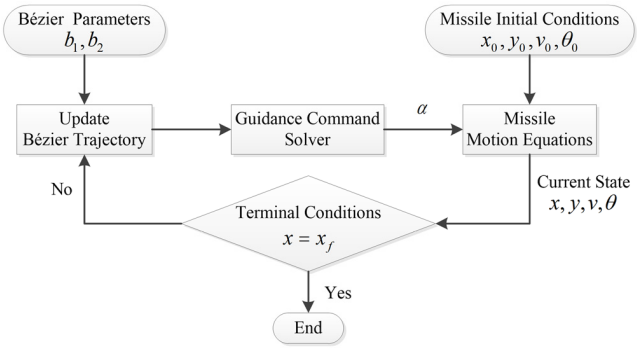

FIGURE 5. Simulation procedure.

TABLE 2. Initial and terminal conditions.

Conditions	Value	Unit
(x_0, y_0)	(0, 50)	m
v_0	300	m/s
θ_0	0	°
(x_f, y_f)	(10000, 0)	m
θ_f	−50, −60, −70, −80	°

TABLE 3. Bézier parameters for different impact angles.

θ_f	b_1	b_2
−50°	0.4360	0.7772
−60°	0.4351	0.7732
−70°	0.4438	0.7811
−80°	0.4898	0.8618

Figs. 6–11 show the simulation results for variations in y-x, y-t, v-t, α-t, n_y-t, and θ-t of the climb-and-dive maneuvering trajectories with different impact angles. Table 4 shows the accurate results.

The simulation results indicate that the proposed method can guide the missile to a stationary target along a climb-and-dive maneuvering trajectory with the expected impact angle. The entire trajectory can be divided into two phases: climbing phase and diving phase.

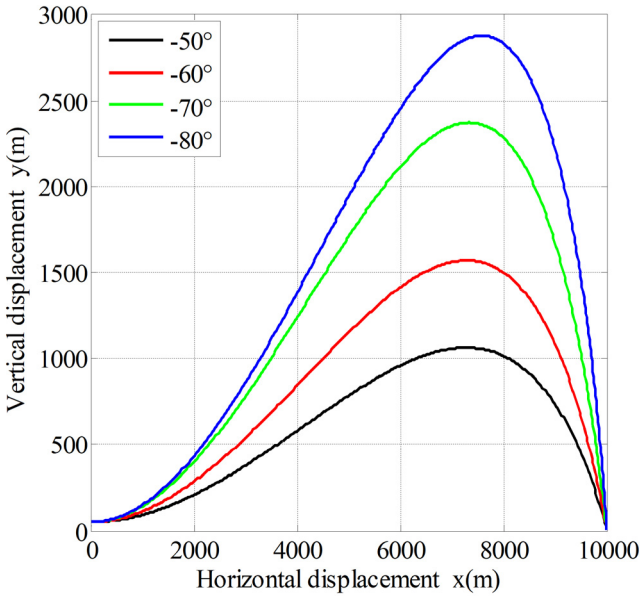

FIGURE 6. Vertical displacement versus horizontal displacement.

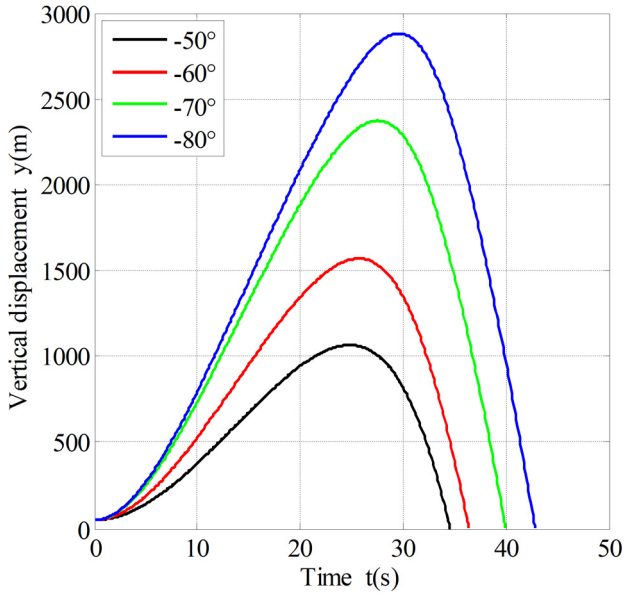

FIGURE 7. Vertical displacement versus time.

TABLE 4. Simulation results.

	−50°	−60°	−70°	−80°
t	34.58s	36.39s	39.97s	42.73s
y_{max}	1063.4m	1570.2m	2374.7m	2880.7m
v_f	334.49m/s	343.17m/s	356.76m/s	365.30m/s
α_{max}	−8.01°	−3.47°	−4.15°	−5.61°
n_{ymax}	−10.01	−4.66	−2.97	−4.70
θ_f	−49.92°	−59.96°	−69.97°	−79.30°

1) FIRST PHASE: CLIMBING

The climbing phase starts from the initial point to the maximum altitude point of the trajectory, as shown in Figs. 6 and 7.

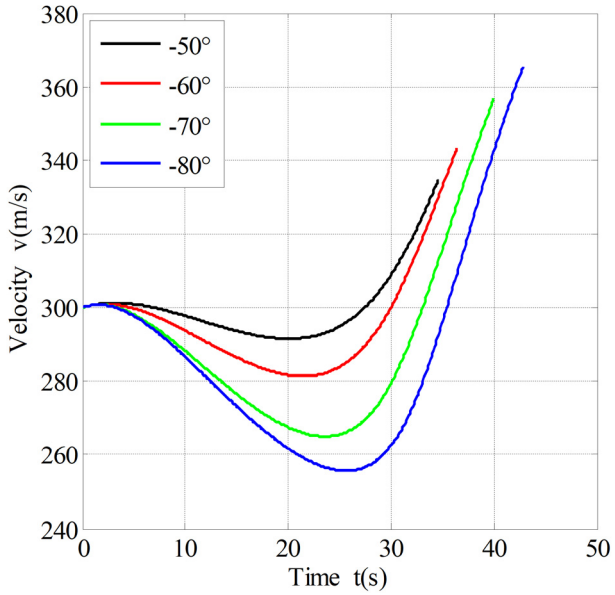

FIGURE 8. Velocity versus time.

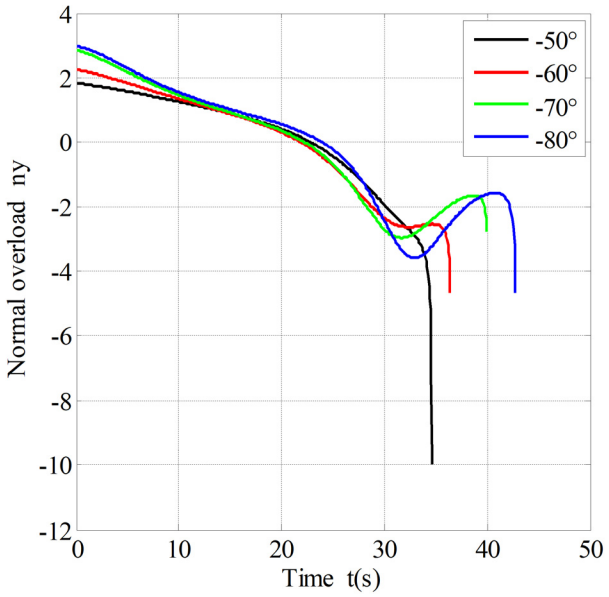

FIGURE 10. Normal overload versus time.

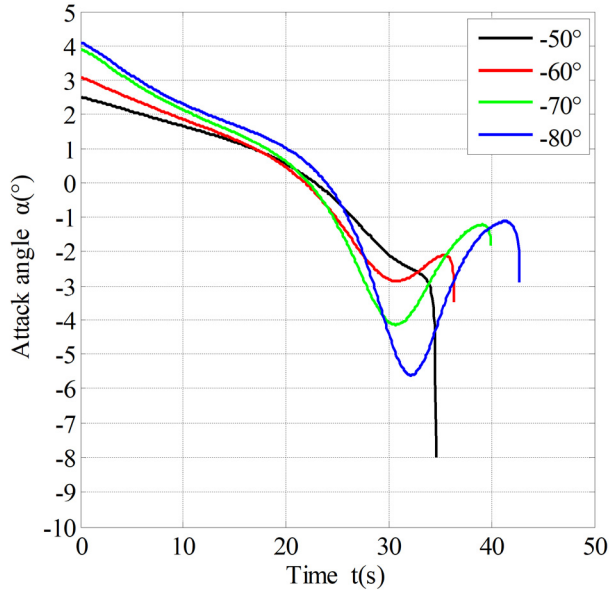

FIGURE 9. Attack angle versus time.

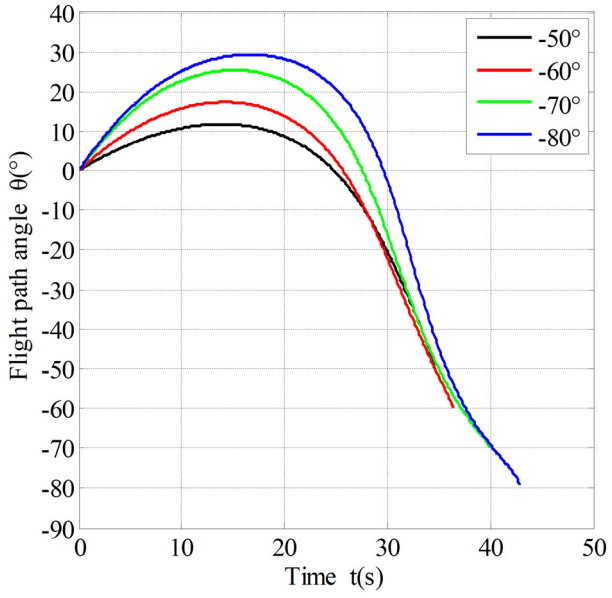

FIGURE 11. Flight path angle versus time.

At the beginning, the missile needs a large normal acceleration when it turns from the horizontal cruising phase to the climbing phase. Thus, the attack angle must be a large positive value to provide a sufficiently large lift, as shown in Fig. 9. The normal overload will also be a large value in pace with the attack angle, as shown in Fig. 10. With the altitude increasing, the missile velocity decreases continuously, as shown in Fig. 8. The flight path angle increases from 0° to the maximum, and then decreases to 0°, as shown in Fig. 11. The attack angle decreases to 0° and then increases negatively, as well as the normal overload, as shown in Figs. 9 and 10. When the missile reaches the maximum altitude point of the trajectory, the climbing phase ends.

2) SECOND PHASE: DIVING

The diving phase starts from the maximum altitude point of the trajectory to the terminal point, as shown in Figs. 6 and 7. At the maximum altitude point, the flight path angle switches from positive to negative, then the missile enters the diving phase. When the derivative of attack angle switches from negative to positive, the attack angle decreases to 0° positively, as well as the normal overload, as shown in Figs. 9 and 10. With the altitude decreasing, the missile velocity increases continuously, as shown in Fig. 8. The flight path angle decreases to the expected impact angle gradually until the missile hits the target, as shown in Fig. 11.

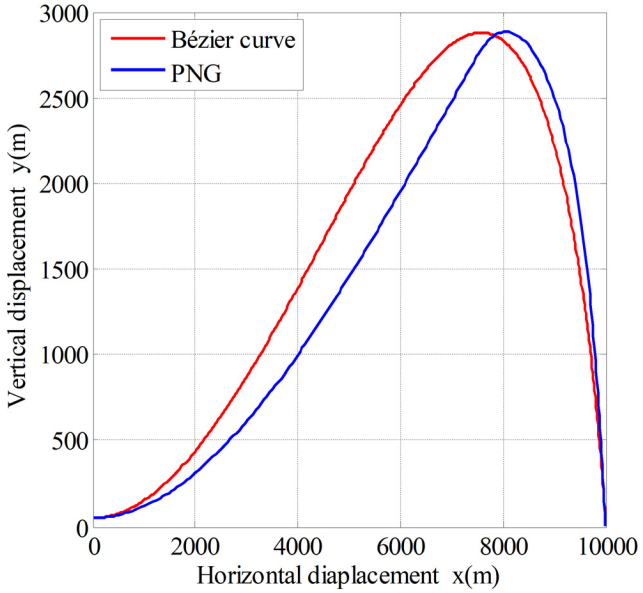

FIGURE 12. Vertical displacement versus horizontal displacement.

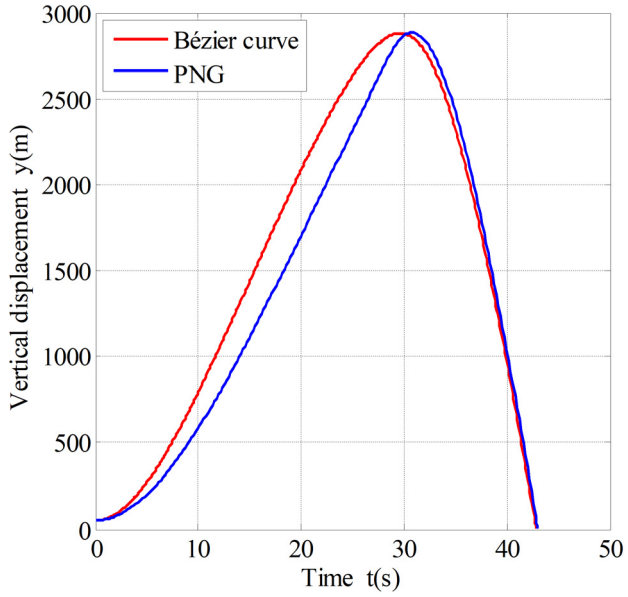

FIGURE 13. Vertical displacement versus time.

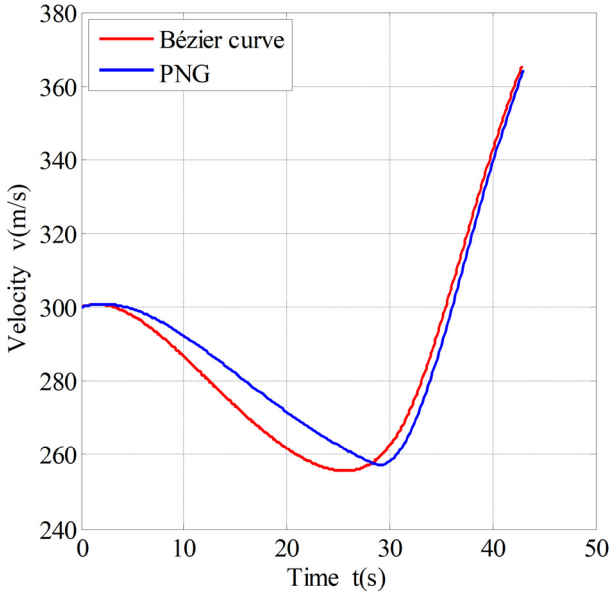

FIGURE 14. Velocity versus time.

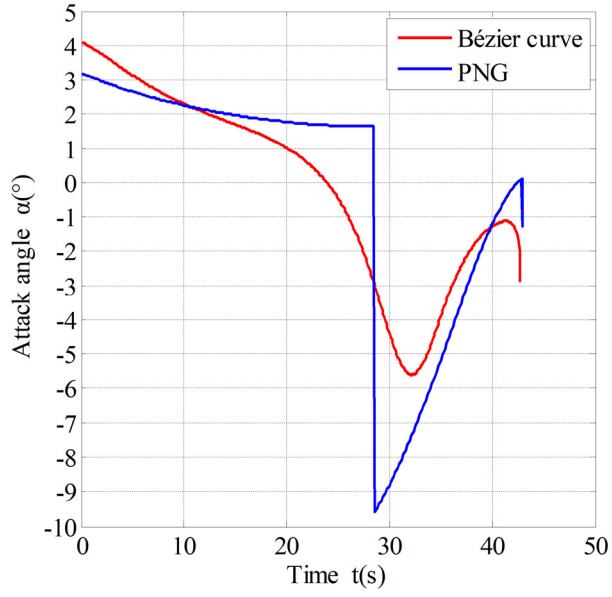

FIGURE 15. Attack angle versus time.

B. COMPARISON WITH TWO-PHASE PNG METHOD

PNG (proportional navigation guidance) is a commonly used method for missile guidance. The angular velocity of flight path angle is proportional to the angular velocity of line-of-sight angle. The curvature of the trajectory is determined by the proportional guidance coefficient K_p. For comparison, a two-phase PNG method is applied to achieve the climb-and-dive maneuvering trajectory with impact angle constraint. Thus, a transition point T (x_T, y_T), which near the highest point of trajectory, is introduced in this method. At the first phase, the missile climbs from the initial point to the transition point. Then at the second phase, the missile dives from the transition point to the terminal point.

The simulation results of Bézier and two-phase PNG methods for a $-80°$ impact angle constraint are shown in Figs. 12–17 and Table 5. Both of the trajectories have the same initial and terminal conditions, as shown in Table 2. The proportional guidance coefficient $K_p = 3.41$, and the coordinate of the transition point is T (7500, 2748).

Comparison results show that both of the guidance methods can implement the climb-and-dive maneuvering trajectory while maintaining the impact angle constraint, as shown in Figs. 12, 13, and 17. However, the two-phase PNG method requires to estimate and regulate the value of K_p and the position of T (x_T, y_T) to meet the expected impact angle. This is a cumbersome procedure, and the value of

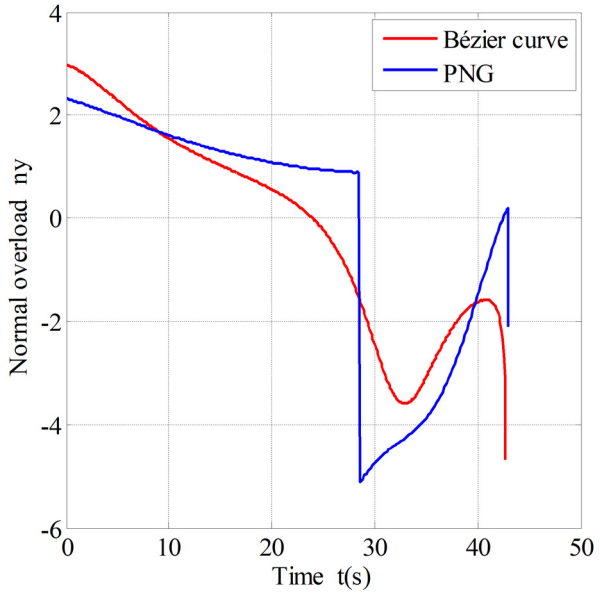

FIGURE 16. Normal overload versus time.

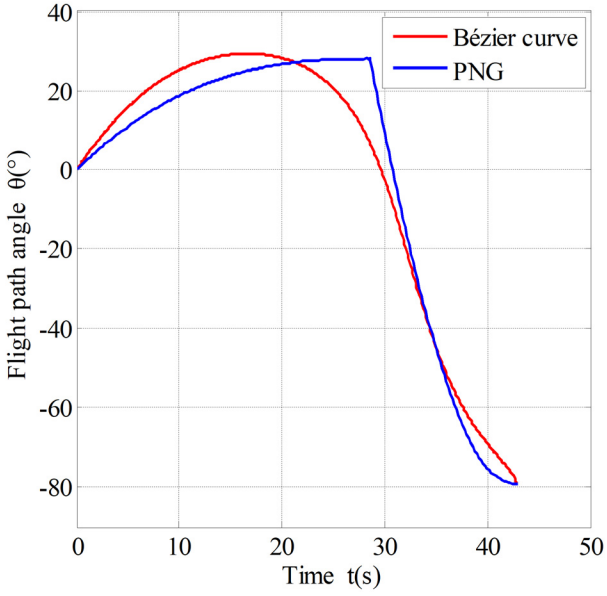

FIGURE 17. Flight path angle versus time.

TABLE 5. Comparison results.

	Bézier trajectory	PNG trajectory
t	42.73 s	42.98 s
$y_{\max}$	2880.7 m	2882.9 m
v_f	365.30 m/s	364.32 m/s
$\alpha_{\max}$	−5.61°	−9.59°
$n_{y\max}$	−4.70	−5.13
θ_f	−79.30°	−79.20°

impact angle is inaccurate. The Bézier method contains the impact angle constraint in its trajectory geometric equations. Thus, the impact angle is maintained accurately. The attack angle and normal overload plots of the proposed Bézier method are smoother than those of the two-phase PNG method. Because the control command varies continuously without mutation. Thus, the proposed Bézier method indicates better performance.

V. CONCLUSIONS

An innovative terminal guidance method is proposed in this paper, which can guide the cruise missile to a stationary target along a climb-and-dive maneuvering trajectory while meeting the expected impact angle. The maneuvering trajectory is shaped by a third-order Bézier curve based on the missile current state, the target position, and the impact angle constraint. Trajectory characteristics, such as shape, altitude, velocity, and flight time, can be modified by regulating the Bézier parameters. Furthermore, the shape of Bézier trajectory is determined by the control points only. The positions of control points are updated in real time. Thus, the control command is updated based on the current Bézier trajectory. That means the proposed method can overcome the initial deviation within a certain range. The simulation results demonstrate the effectiveness of the proposed method in terminal guidance.

REFERENCES

[1] I.-S. Jeon, J.-I. Lee, and M.-J. Tahk, "Impact-time-control guidance law for anti-ship missiles," *IEEE Trans. Control Syst. Technol.*, vol. 14, no. 2, pp. 260–266, Mar. 2006.
[2] M. Kim and K. V. Grider, "Terminal guidance for impact attitude angle constrained flight trajectories," *IEEE Trans. Aerosp. Electron. Syst.*, vol. AES-9, no. 6, pp. 852–859, Nov. 1973.
[3] X. Wang, Y. Zhang, and H. Wu, "Distributed cooperative guidance of multiple anti-ship missiles with arbitrary impact angle constraint," *Aerosp. Sci. Technol.*, vol. 46, pp. 299–311, Oct./Nov. 2015.
[4] A. Ratnoo and D. Ghose, "Impact angle constrained guidance against nonstationary nonmaneuvering targets," *J. Guid., Control, Dyn.*, vol. 33, no. 1, pp. 269–275, Jan. 2010.
[5] A. Ratnoo and D. Ghose, "Impact angle constrained interception of stationary targets," *J. Guid., Control, Dyn.*, vol. 31, no. 6, pp. 1817–1822, 2008.
[6] A. Ratnoo, "Analysis of two-stage proportional navigation with heading constraints," *J. Guid., Control, Dyn.*, vol. 39, no. 1, pp. 156–164, 2016.
[7] A. Farooq and D. J. N. Limebeer, "Trajectory optimization for air-to-surface missiles with imaging radars," *J. Guid., Control, Dyn.*, vol. 25, no. 5, pp. 876–887, 2002.
[8] S. Subchan and R. Żbikowski, "Computational optimal control of the terminal bunt manoeuvre—Part 1: Minimum altitude case," *Optim. Control Appl. Methods*, vol. 28, no. 5, pp. 311–353, 2007.
[9] S. Subchan and R. Żbikowski, "Computational optimal control of the terminal bunt manoeuvre—Part 2: Minimum-time case," *Optim. Control Appl. Methods*, vol. 28, no. 5, pp. 355–379, 2007.
[10] D. M. K. K. V. Rao and T. H. Go, "Optimization, stability analysis, and trajectory tracking of perching maneuvers," *J. Guid., Control, Dyn.*, vol. 37, no. 3, pp. 879–888, 2014.
[11] B. S. Kim, J. G. Lee, and H. S. Han, "Biased PNG law for impact with angular constraint," *IEEE Trans. Aerosp. Electron. Syst.*, vol. 34, no. 1, pp. 277–288, Jan. 1998.
[12] T.-H. Kim, B.-G. Park, and M.-J. Tahk, "Bias-shaping method for biased proportional navigation with terminal-angle constraint," *J. Guid., Control, Dyn.*, vol. 36, no. 6, pp. 1810–1816, 2013.
[13] C.-H. Lee, T.-H. Kim, and M.-J. Tahk, "Interception angle control guidance using proportional navigation with error feedback," *J. Guid., Control, Dyn.*, vol. 36, no. 5, pp. 1556–1561, Sep./Oct. 2013.
[14] Y. A. Zhang, G. X. Ma, and H. L. Wu, "A biased proportional navigation guidance law with large impact angle constraint and the time-to-go estimation," *Proc. Inst. Mech. Eng. G, J. Aerosp. Eng.*, vol. 228, no. 10, pp. 1725–1734, 2014.

[15] C. H. Lee, T. H. Kim, M. J. Tahk, and I. H. Whang, "Polynomial guidance laws considering terminal impact angle and acceleration constraints," *IEEE Trans. Aerosp. Electron. Syst.*, vol. 49, no. 1, pp. 74–92, Jan. 2013.
[16] C.-K. Ryoo, H. Cho, and M.-J. Tahk, "Optimal guidance laws with terminal impact angle constraint," *J. Guid., Control, Dyn.*, vol. 28, no. 4, pp. 724–732, 2005.
[17] C.-K. Ryoo, H. Cho, and M.-J. Tahk, "Time-to-go weighted optimal guidance with impact angle constraints," *IEEE Trans. Control Syst. Technol.*, vol. 14, no. 3, pp. 483–492, May 2006.
[18] C. Chawla, P. Sarmah, and R. Padhi, "Suboptimal reentry guidance of a reusable launch vehicle using pitch plane maneuver," *Aerosp. Sci. Technol.*, vol. 14, no. 6, pp. 377–386, 2010.
[19] A. Maity, H. B. Oza, and R. Padhi, "Generalized model predictive static programming and angle-constrained guidance of air-to-ground missiles," *J. Guid., Control, Dyn.*, vol. 37, no. 6, pp. 1897–1913, 2014.
[20] S. He, D. Lin, and J. Wang, "Continuous second-order sliding mode based impact angle guidance law," *Aerosp. Sci. Technol.*, vol. 41, pp. 199–208, Feb. 2015.
[21] S. R. Kumar, S. Rao, and D. Ghose, "Sliding-mode guidance and control for all-aspect interceptors with terminal angle constraints," *J. Guid., Control, Dyn.*, vol. 35, no. 4, pp. 1230–1246, 2012.
[22] S. R. Kumar, S. Rao, and D. Ghose, "Nonsingular terminal sliding mode guidance with impact angle constraints," *J. Guid., Control, Dyn.*, vol. 37, no. 4, pp. 1114–1130, 2014.
[23] K. G. Jolly, R. S. Kumar, and R. Vijayakumar, "A Bezier curve based path planning in a multi-agent robot soccer system without violating the acceleration limits," *Robot. Auto. Syst.*, vol. 57, no. 1, pp. 23–33, 2009.
[24] H. Zhou, T. Rahman, and W. C. Chen, "Impact angle and impact velocity constrained terminal guidance for stationary target," *Aircr. Eng. Aerosp. Technol., Int. J.*, vol. 87, no. 5, pp. 454–464, 2015.

ZHEN QIN received the B.S. degree in aircraft design and engineering from Beihang University, Beijing, China, in 2013, where he is currently pursuing the Ph.D. degree in mechatronic engineering. His research interests include aircraft design, aircraft guidance, and aircraft hydraulic transmission and control.

XIAOYE QI received the Ph.D. degree in mechatronic engineering from Yanshan University, Qinhuangdao, China, in 1998. He is currently an Associate Professor with the School of Mechanical Engineering and Automation, Beihang University. His research interests include aircraft hydraulic transmission and control, and electromechanical system control.

YONGLING FU received the Ph.D. degree in mechanical engineering from the Harbin Institute of Technology, China, in 1993. He is currently a Professor with the School of Mechanical Engineering and Automation, Beihang University. His research interests include mechatronics, aircraft hydraulic transmission and control, and integrated electro-hydraulic system control.